Nephrol Dial Transplant (2018) 33: ii29–ii40
doi: 10.1093/ndt/gfy163

ndt
Nephrology Dialysis Transplantation

Diffusion-weighted magnetic resonance imaging to assess diffuse renal pathology: a systematic review and statement paper

Anna Caroli[1], Moritz Schneider[2,3], Iris Friedli[4], Alexandra Ljimani[5], Sophie De Seigneux[6], Peter Boor[7], Latha Gullapudi[8], Isma Kazmi[8], Iosif A. Mendichovszky[9], Mike Notohamiprodjo[10], Nicholas M. Selby[8], Harriet C. Thoeny[11], Nicolas Grenier[12] and Jean-Paul Vallée[4]

[1]Medical Imaging Unit, Bioengineering Department, IRCCS Istituto di Ricerche Farmacologiche Mario Negri, Bergamo, Italy, [2]Department of Radiology, Ludwig-Maximilians-University Hospital Munich, Munich, Germany, [3]Comprehensive Pneumology Center, German Center for Lung Research, Munich, Germany, [4]Division of Radiology, Geneva University Hospitals, University of Geneva, Geneva, Switzerland, [5]Department of Diagnostic and Interventional Radiology, Medical Faculty, University Dusseldorf, Dusseldorf, Germany, [6]Service and Laboratory of Nephrology, Department of Internal Medicine Specialties and Department of Physiology and Metabolism, Geneva University Hospitals, University of Geneva, Geneva, Switzerland, [7]Institute of Pathology and Division of Nephrology, RWTH University of Aachen, Aachen, Germany, [8]Centre for Kidney Research and Innovation, University of Nottingham, Nottingham, UK, [9]Department of Radiology, Cambridge University Hospitals NHS Foundation Trust, Addenbrooke's Hospital, Cambridge, UK, [10]Department of Radiology, University Hospital Tuebingen, Tuebingen, Germany, [11]Department of Diagnostic, Pediatric, and Interventional Radiology, Inselspital University Hospital, Bern, Switzerland and [12]Service d'Imagerie Diagnostique et Interventionnelle de l'Adulte, Centre Hospitalier Universitaire de Bordeaux, Bordeaux, France

Correspondence and offprint requests to: Jean-Paul Vallée; E-mail: jean-paul.vallee@unige.ch; Twitter handle: @renalMRI

ABSTRACT

Diffusion-weighted magnetic resonance imaging (DWI) is a non-invasive method sensitive to local water motion in the tissue. As a tool to probe the microstructure, including the presence and potentially the degree of renal fibrosis, DWI has the potential to become an effective imaging biomarker. The aim of this review is to discuss the current status of renal DWI in diffuse renal diseases. DWI biomarkers can be classified in the following three main categories: (i) the apparent diffusion coefficient—an overall measure of water diffusion and microcirculation in the tissue; (ii) true diffusion, pseudodiffusion and flowing fraction—providing separate information on diffusion and perfusion or tubular flow; and (iii) fractional anisotropy—measuring the microstructural orientation. An overview of human studies applying renal DWI in diffuse pathologies is given, demonstrating not only the feasibility and intra-study reproducibility of DWI but also highlighting the need for standardization of methods, additional validation and qualification. The current and future role of renal DWI in clinical practice is reviewed, emphasizing its potential as a surrogate and monitoring biomarker for interstitial fibrosis in chronic kidney disease, as well as a surrogate biomarker for the inflammation in acute kidney diseases that may impact patient selection for renal biopsy in acute graft rejection. As part of the international COST (European Cooperation in Science and Technology) action PARENCHIMA (Magnetic Resonance Imaging Biomarkers for Chronic Kidney Disease), aimed at eliminating the barriers to the clinical use of functional renal magnetic resonance imaging, this article provides practical recommendations for future design of clinical studies and the use of renal DWI in clinical practice.

Keywords: chronic kidney disease, diffuse renal pathology, diffusion-weighted MRI, fibrosis, functional MRI

INTRODUCTION

Assessment of renal microstructure is an important step for the diagnosis and monitoring of renal diseases and it is currently performed by renal biopsy, an invasive procedure carrying the risk of side effects and sampling bias.

Diffusion-weighted magnetic resonance imaging (DWI) is a non-invasive method to assess the displacement of the water molecules in tissue including Brownian motion. Current evidence suggests that DWI is particularly sensitive to alterations in the renal interstitium, e.g. during renal fibrosis, cellular (inflammatory or tumorous) infiltration or oedema, in renal perfusion and in water handling in the tubular compartment. Intensive ongoing research efforts are aimed at unveiling the potential of DWI as an imaging biomarker for renal diseases,

with the most promising results in fibrosis estimation in chronic kidney disease (CKD) and in biopsy guidance in acute graft dysfunction.

The present article, coming from the clinical working group of the COST (European Cooperation in Science and Technology) action PARENCHIMA (Magnetic Resonance Imaging Biomarkers for Chronic Kidney Disease) (www.renalmri.org), aims to review all the existing literature on DWI in well-functioning kidneys and kidneys with diffuse renal pathologies, to discuss the current status of renal DWI as an imaging biomarker, and to provide practical recommendations that could be useful to design future clinical studies as well as to use DWI in clinical practice.

METHODOLOGY (INCLUSION AND EXCLUSION CRITERIA)

A comprehensive search for all the DWI studies in human subjects or patients related to the kidneys and excluding cancer studies or animal experiments was performed on 30 August 2017 using PubMed, and crossed checked with references cited by the related publications. Search terms are available as Supplementary data (Section S2). A total of 399 hits were found, identifying 172 papers meeting the inclusion criteria. All the human studies involving renal DWI have been summarized in tables and are available as Supplementary data (see Supplementary review table), along with technical details, to facilitate further research in this field.

RENAL DWI ACQUISITION AND ANALYSIS

Pulse sequences and readout techniques

In DWI, image contrast is based on the displacement of water molecules, whereby mobile molecules appear hypointense. This is achieved by employing magnetic field gradients of varying strength during the acquisition, generating images with varying degrees of diffusion-weighting, referred to as *b*-values. The signal decrease as a function of the *b*-value can then be analysed using model functions ('DWI models' section) to quantify the water displacement (Figure 1). The range of motion measured by DWI is typically in the order of 1–17 μm [1]. A key element for successful DWI is the use of very fast magnetic resonance sequences minimizing the signal from organ motion during the acquisition, such as echo-planar imaging (EPI) with fat suppression [2] (stated in 61.7% of reviewed studies). To further reduce the acquisition time, acceleration methods are frequently added and these are of great research interest.

Renal DWI is performed in either the axial or coronal image orientation. A coronal orientation provides easier full kidney coverage but is more prone to respiratory motion. Ways to mitigate respiratory motion during data acquisition comprise physiological triggering of the pulse sequence (stated in 38.3%), performing breath-hold acquisitions (stated in 18.2%) or free breathing with multiple acquisitions.

Even though DWI biomarkers are quantitative, the applied diffusion-weighting strategy will affect the final parameter estimates and it thus needs to be tailored to the intended DWI biomarker. This includes the strength and the number of the different diffusion weightings, as well as the diffusion gradient directions, since the molecular diffusion in the kidneys is of an anisotropic nature (meaning spatially oriented), especially within medulla.

While the literature [3–5] is divided about the effect of a subject's hydration status on DWI biomarkers, we recommend controlling the hydration status by hydrating the patients prior to DWI, to eliminate this potential confounder.

Please refer to Table 1 for practical recommendations and to Section S3.1 (Supplementary data) for technical details on DWI acquisition.

Renal DWI processing

There is great heterogeneity in the DWI processing pipelines and in the software tools used to correct the motion, segment the kidneys, draw the regions of interest (ROIs) and fit the model of choice (Supplementary data, Section S3.4).

DWI parameter computation is affected by image quality [6]. A careful visual inspection beforehand (to identify possible artefacts and eventually exclude problematic images) is needed, along with motion correction (which to date has been performed only in a minority of cases), to have reliable diffusion parameter maps and quantitative results.

A variety of ROIs have been used to quantify DWI parameters either in the entire kidney or separately in cortex and medulla. Vascular structures, collecting system, tissue boundaries, artefacts, areas of heterogeneous signal intensity, cysts and lesions potentially affecting the average values should be avoided. ROIs should be placed in the upper pole, lower pole and mid-level in homogenous areas of the kidneys to have representative average values, or in hyper- and hypointense areas in case of heterogenous kidneys.

A number of software tools are available to compute DWI biomarkers by fitting appropriate signal attenuation models. The software choice is determined by the model complexity and the biomarkers sought (Supplementary data, Section S3.4).

RENAL DWI BIOMARKERS

All DWI models and biomarkers are summarized in Table 2.

DWI models

In free water, DWI signal resulting from water motion exponentially decays with the strength of the magnetic gradient applied (*b*-value) [7]. However, in renal tissue, molecular water motion is not free but hindered by many obstacles such as cell membranes and interstitial matrix and influenced by water handling. To account for this, in the tissue, diffusion is called 'apparent', and DWI signal decay can be described by a mono-exponential equation (Supplementary data, Section S3.2).

The apparent diffusion coefficient (ADC) is usually averaged from three spatial directions of signal encoding to take into account the renal anisotropy and therefore to avoid under- or overestimation.

Beyond water diffusion in the tissue, apparent motion also results from blood microcirculation and from tubular flow, which may be viewed as pseudodiffusion processes mimicking diffusion and impacting DWI measurements. Like diffusion,

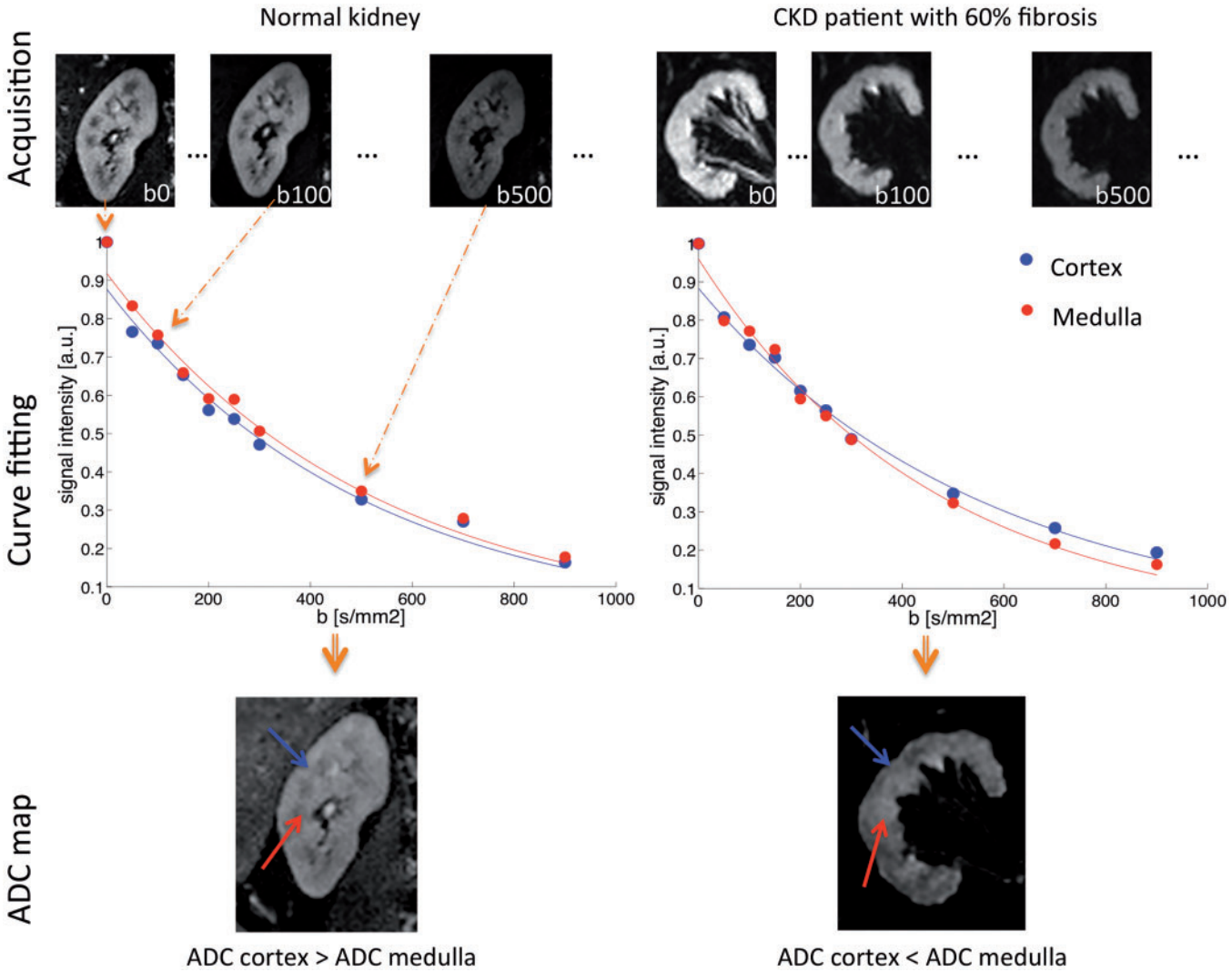

FIGURE 1: Illustration of the principles of renal DWI in a normal volunteer and a CKD patient with 60% of renal fibrosis. First, a series of renal MRI with varying degrees of diffusion weighting are acquired as shown in the first row. Then, the ADC, an estimation of the water molecule motion in the tissue, is extracted from these images by curve fitting. An example of the ADC fit is presented in the graphs in the middle row. Note the difference in the cortical and medulla fits between the normal volunteer without fibrosis and the CKD patient. The medulla curve in the CKD patient has a stronger curvature reflecting an increased ADC. Finally, the result of fit for each pixel is displayed in a new image called an ADC map (bottom row). In the normal volunteer (on the left), the ADC is higher in the cortex (blue arrow) than in the medulla (red arrow). The opposite is found in the CKD patient (on the right), where the ADC is higher in the medulla than in the cortex in agreement with the curve fits. This inversion of cortico-medullary ADC difference is correlated with the amount of fibrosis present in the CKD patient.

blood microcirculation results in a monoexponential decay of the magnetic resonance imaging (MRI) signal, but 10 times faster, which results in a biexponential decay of diffusion signal. This model allows to calculate, apart from ADC, the pseudodiffusion (D*), the flowing fraction within blood vessels and tubuli (F) and the true water diffusion coefficient in the tissue (D).

This intra-voxel incoherent motion (IVIM) model describes DWI data at best, in the presence of sufficient signal-to-noise ratio (SNR) [8] (Supplementary data, Section S3.2). On the contrary, the monoexponential model is the most robust against low SNR but fits DWI data the least [8–10]. Despite the number of studies showing its limitations, monoexponential model has still been used in the majority of renal DWI studies performed so far (68% in total, reducing to 50% of the studies performed since 2016), probably due to the wide availability and ease of use of ADC (but not IVIM parameter) computation tools.

Encoding the diffusion signal in a greater number of directions makes it possible to investigate the spatial dependence of diffusion, to quantify the degree of tissue anisotropy and, consequently, to characterize the tissue microarchitecture: this advanced method is called diffusion tensor imaging (DTI). DTI requires multiple measurements with at least six different diffusion-sensitizing directions of signal encoding [11]. DTI analysis allows assessment of the fractional anisotropy (FA), which is the percentage of spatially oriented diffusion signal, reflecting the degree of tissue anisotropy (0% = complete isotropy; 100% = complete anisotropy). Consequently, the mean diffusivity (MD), an anisotropy-independent ADC equivalent,

Table 1. DWI in the kidney: key aspects

Patient preparation	
Hydration	Potential confounder Control by hydrating the patient whenever possible
Data acquisition	
Echo time	Minimize to optimize SNR Minimum limited by maximum *b*-value
Repetition time	Long enough to allow for T1 relaxation (>1500 ms) Minimum limited by number of image slices
Image orientation	Axial: less motion in image plane Coronal: easier full kidney coverage
Field of view	Usually covers the entire abdomen (320–400 mm) *Z*-dimension dependent on image orientation
Resolution	Increase: sharpness$_{\uparrow}$ partial volume effects$_{\downarrow}$ Decrease: ETL$_{\downarrow}$ kidney coverage$_{\uparrow}$ SNR$_{\uparrow}$
ETL	Shorten to lessen susceptibility artefacts Measures: parallel imaging, multi-shot EPI, partial Fourier
Motion compensation	Physiological triggering using external devices Intrinsic triggering using MRI signal (navigator)
b-values	Tailor to respective DWI biomarker Increase number to improve parameter estimates
Image post-processing	
Image quality control	Discard problematic image(s) to ensure imaging parameter value reliability
Motion correction	To account for motion artefacts and eddy current-induced deformations
ROI definition (kidney/medulla/cortex)	From more than one section to have representative average values; no vessels, artefacts, lesions
Model fitting	To compute DWI biomarkers by fitting appropriate signal attenuation models

EPI, echo-planar imaging; ETL, echo train length; MRI, magnetic resonance imaging; SNR, signal to noise ratio

Table 2. DWI biomarker estimation models to investigate renal tissue microstructure

Model	Biomarker(s)	Pros (+) and cons (−)
Monoexponential	ADC: apparent diffusion in the tissue	+ Most robust against noise + Wide availability and ease of use of biomarker estimation tools − Provides limited information (apparent diffusion only) − Fits DWI data the least
IVIM	D: water diffusion in the tissue D*: pseudodiffusion F: flowing fraction	+ Describes DWI signal attenuation at best provided sufficient signal-to-noise + Can separate diffusion from pseudodiffusion − No standardized algorithm to compute IVIM parameters
DTI	FA: fractional anisotropy diffusion anisotropy imposed by the tissue microstructure MD: anisotropy-independent mean diffusivity	+ Provides information on tissue anisotropy − Requires a dedicated acquisition sequence (DTI) with multiple directions
Extended IVIM	D: water diffusion in the tissue D*: pseudodiffusion F: flowing fraction Additional model-specific biomarkers	+ Potentially advances the characterization of the renal microstructure and microcirculation − Requires complex biomarker estimation − Need further investigation, especially in pathological kidneys
Non-Gaussian	ADC: apparent diffusion in the tissue K/σ/δ: measure of the degree of deviation of diffusion from a Gaussian law	+ Accounts for the complexity of diffusion in the renal tissue − Requires complex biomarker estimation − Fits DWI data better than monoexponential but worse than IVIM model

can also be measured (see Section S3.3, Supplementary data, for additional details). All DTI studies reported a higher degree of anisotropy within the medulla than within the cortex [5, 9, 12–19] presumably due to predominant water motion along tubular and vascular bundles of pyramids [20, 21].

More complex models have been recently proposed (see Section S3.2, Supplementary data), but despite their potential, further studies in particular in diseased kidneys are needed to understand their advantage over the commonly used models described above.

Renal DWI biomarkers validation and qualification

Discovery. Following the success of DWI in the brain, the feasibility of DWI in the kidney has been well demonstrated in both experimental and clinical settings (see Supplementary review table). Renal DWI biomarkers, computed using the well-established methodologies described above, have been widely adopted, although novel DWI acquisition and modelling methods are constantly proposed (see Section S3.2, Supplementary data).

Biological validation. Despite DWI potential being well recognized, the specific confirmation of mechanisms and processes measured by DWI is not yet clearly established. This is mainly due to the absence of a gold standard to measure *in vivo* renal diffusion. Renal perfusion [22], glomerular and tubular flow [23, 24] as well as water handling [18] can all modify the DWI signal and induce changes in the ADC. Therefore, the multifactorial dependence of the DWI contrast complicates the understanding of its origin and probably decreases the specificity of the observed value changes. A reduction of perfusion and tubular flow as well as the extracellular space by cellular infiltration could explain the decreased ADC observed in some acute kidney diseases, such as acute cellular graft rejection [25] or acute pyelonephritis (APN) [26]. The situation is also complex in case of renal fibrosis. Intuitively, and as demonstrated by simulation and phantom experiments [27], deposition of fibrotic matrix in the interstitial space is expected to decrease the Brownian motion of the water molecules by collision, in addition to the reduced perfusion and tubular flow, which is often also present. Several studies have consistently demonstrated a negative correlation between the renal ADC and the amount of renal fibrosis in CKD [23, 24, 28]. Of interest, an experimental study of renal fibrosis in rats suggested that this correlation was merely due to the reduction of renal perfusion and glomerular filtration rather than directly because of the fibrotic matrix deposition [29]. Whether these results, based on the observation of a post-mortem ADC increase with renal fibrosis, can be translated to the *in vivo* setting remains to be further investigated. In this respect, the ability of advanced modelling of the diffusion signal using the IVIM model to separate the effects of flowing fraction from the Brownian motion or DTI to probe the structure orientation, may significantly improve our understanding of the diffusion mechanism.

Technical validations. Numerous reproducibility studies have been conducted with either the monoexponential, the biexponential (i.e. IVIM) or the DTI model. Regarding the acquisition, a variation coefficient of $<10\%$ was measured in 10 volunteers examined successively on magnetic resonance scanner from several vendors [30]. Good inter- or intra-observer reproducibility were also reported for the DWI analysis of the kidneys [24]. However, the variations in ADC values and other diffusion-related parameters remain large. An absence of standardized acquisition and analysis protocol may explain such variation reported in the literature (Supplementary data, Tables S1, S2 and S3). A significant effort of standardization is needed to define DWI accuracy and bias.

Qualification. No renal DWI qualification studies have been performed so far, i.e. studies demonstrating the clinical benefit of DWI in diagnosis, treatment decision or outcome that would be required for regulatory acceptance of DWI as biomarker. However, some preliminary studies have shown the potential of DWI to predict the need for therapy modification [31, 32].

RENAL DWI AS IMAGING BIOMARKER IN CLINICAL PRACTICE

Acute graft dysfunction

DWI in transplanted kidneys has shown promising results in detecting allografts with impaired renal function based on the lower ADC values, lower medullary FA and lower medullary flowing fraction F compared with normal renal allografts [33–37] (Table 3). Although the ADC values were significantly lower in transplanted kidneys with acute rejection (AR), acute tubular necrosis (ATN) and immunosuppressive toxicity compared with healthy renal allografts, DWI was unable to differentiate the various underlying pathologies responsible for the impaired renal function. However, heterogeneous appearance of DWI is a morphological sign associated with severe underlying histopathological changes [32, 57]. Therefore, a combination of qualitative and quantitative analysis of DWI parameters might further improve the assessment of the severity of renal allograft dysfunction and might be helpful in the management of these patients to decide when to perform biopsy [32].

APN

DWI was shown to be more sensitive than sonography to detect the infected renal segments during APN. With a simple qualitative analysis, in combination with clinical information, DWI could have a significant clinical impact on confirming the treatment effectiveness during follow-up, mainly in children and in pregnant women [59–61]. Furthermore, abscesses as a potential complication of pyelonephritis can be differentiated from a cyst by DWI showing restricted diffusion and cystic appearance on morphological images. In summary, DWI allows detection of renal infection in adults, children and transplanted kidneys based on the qualitative analysis of DWI data and it can also be applied for treatment monitoring. In this indication, DWI may replace contrast-enhanced MRI, avoiding potential contrast agent side effects.

Polycystic disease

In patients with polycystic kidney disease suspicious for cyst complication, a high intracystic signal intensity on DWI showed a sensitivity of 86.4% for intracystic infection, but its specificity was low, with similar findings observed in intracystic haemorrhage [62].

To our knowledge, only one preliminary pilot study tried to evaluate several functional sequences, including IVIM, within non-cystic renal parenchyma (NCRP) of polycystic kidneys, compared with age-matched controls [63]. Among several other parameters, higher ADCs, higher pure diffusion and lower flowing fraction were reported in NCRP. ADC values were also correlated with height-adjusted total kidney volume

Table 3. Renal DWI applications in chronic kidney disease and kidney allograft dysfunction

Disease group	Study	Sample size (n)	Age (years)	Histology	Aetiology	Renal dysfunction severity	Diffusion biomarkers	Main results
CKD	Inoue (2011) [38]	119	52 ± 18	Yes	No diabetes ($n = 76$), diabetes ($n = 43$)	Mean eGFR= 45 ± 30; CKD G1-5, A1-3	ADC, (BOLD)	ADC as accurate index for evaluating renal tubulointerstitial alterations in the cortex
	Li (2014) [39]	71	41 ± 12	Yes	Lupus nephritis	CKD G1-5, AX	ADC	ADC reflected the severity of renal pathology
	Liu (2015) [40]	51	35 ± 14	Yes	Minor glomerular abnormalities ($n = 5$), IgA nephropathy ($n = 12$), membranous nephropathy ($n = 20$), crescentic glomerulonephritis ($n = 1$), lupus nephritis ($n = 5$), anaphylactic purpura nephritis ($n = 3$), focal segmental glomerulosclerosis ($n = 2$), hypertensive renal damage ($n = 1$), hepatitis B virus-associated glomerulonephritis ($n = 2$)	eGFR = NA; CKD G1-4, AX	ADC, FA	Renal parenchymal FA correlated with renal function and pathological changes
	Rona (2016) [41]	20	50 ± 18	Yes	Renal amyloidosis	Mean eGFR NA, only eGFR > 60; CKD G3-5, AX	ADC	DWI is a useful and non-invasive tool in the diagnosis of secondary renal amyloidosis and differentiating renal amyloidosis from other CKD
	Wang (2014) [42]	29	36 (20–50)	Yes	Mixed CKD	Mean eGFR = 116 ± 13 (CKD1, $n = 5$), 77 ± 10 (CKD2, $n = 6$), 37 ± 9 (CKD3, $n = 7$), 16 ± 2 (CKD4, $n = 4$), 7 ± 3 (CKD5, $n = 7$); CKD G1-5, AX	ADC, FA	Cortical and medullary ADC and FA inversely correlated with serum creatinine and blood urea nitrogen. No difference in ADC and FA between right and left kidneys
	Zhao (2014) [28]	35	42 ± 17	Yes	Membranous nephropathy ($n = 6$), minimal change nephropathy ($n = 5$), atypical membranous nephropathy ($n = 5$), focal proliferative IgA nephropathy ($n = 5$), mesangial proliferative glomerulonephritis ($n = 3$), hypertensive nephropathy ($n = 1$); unknown ($n = 10$)	Mean eGFR between 80 and 120 according to pathology group; CKD GX, AX	ADC	ADC strongly correlated with histological measures of fibrosis
	Ding (2016) [43]	44	54 ± 13	No	Mixed CKD	Mean eGFR= 18 ± 7 (sRI, $n = 25$), 60 ± 25 (non-sRI, $n = 19$); CKD G1-5, A1-3	ADC	ADC linearly related with eGFR
	Ding (2016) [44]	54	53 ± 13	No	Mixed CKD	Mean eGFR= 17 ± 7 (sRI, $n = 25$), 65 ± 26 (non-sRI, $n = 19$); CKD G1-5, A2-3	ADC, D, D*, F	ADC and D positively related with eGFR

	Emre (2016) [45]	62	57 ± 10	No	Diabetes mellitus ($n = 26$), hypertension ($n = 19$), chronic glomerulonephritis ($n = 7$), unknown ($n = 10$)	Mean srCr = 237 ± 167 CKD G1-5 AX	ADC	ADC significantly correlated with CKD clinical stage
	Ichikawa (2013) [46]	365	67 (13–92)	No	Patient undergoing abdominal MRI	eGFR = NA; CKD G1-5, AX	ADC, D, D*, F	As renal dysfunction progresses, renal perfusion might be reduced earlier and affected more than diffusion in renal cortex
	Li (2013) [47]	42	42 ± 12	No	Mixed CKD	Mean GFR = 119 ± 22 (CKD1, $n = 22$), 76 ± 9 (CKD2, $n = 9$), 45 ± 10 (CKD3, $n = 8$), 22 ± 3 (CKD4, $n = 3$); CKD G1-4, AX	ADC	ADC significantly correlated with GFR
	Prasad (2015) [48]	30	62 ± 10	No	Diabetes ($n = 11$), hypertension ($n = 7$), interstitial nephritis ($n = 3$), lupus nephritis ($n = 2$), IgA nephropathy ($n = 1$), membranous glomerulopathy ($n = 1$), cardio-renal syndrome ($n = 1$), unknown ($n = 4$)	Mean eGFR = 43 ± 23; CKD G2-5, AX	ADC	When matched for age and sex, ADC significantly correlated with eGFR
	Xu (2010) [49]	43	36 (18–59)	No	Chronic glomerulonephritis	eGFR NA; CKD G1-5, AX	ADC	DWI is feasible in the assessment of renal function, especially in the detection of early-stage renal failure of CKD
CKD and diabetes	Cakmak (2014) [50]	78	(26–70)	No	Type 2 diabetes	Mean eGFR NA; CKD G1-5, AX	ADC	ADC significantly correlated with clinical stages of diabetic nephropathy
	Chen (2014) [51]	30	57 (38–73)	No	Type 2 diabetes	Normal renal function; CKD G1, A1-2	ADC, FA	Combined ADC and FA values may provide a better quantitative approach for identifying diabetic nephropathy at early disease stage
	Razek (2017) [52]	42	55 (47–60)	No	Type 2 diabetes	Mean srCr = 88 (61–194); CKD G1-5, A1-3	ADC, FA	Cortical FA and ADC help to differentiate diabetic kidney from volunteers, may predict the presence of macroalbuminuria, correlate with urinary and serum biomarkers for diabetes
Kidney allograft: chronic disease	Friedli (2016) [24]	29	54 ± 14	Yes	Transplant	Mean GFR = 48 ± 23; CKD G1-4, A1-3	ADC	DWI can evaluate fibrosis in kidney allograft recipients and allows differentiation of the cortex and medulla

Continued

Table 3. Continued

Disease group	Study	Sample size (*n*)	Age (years)	Histology	Aetiology	Renal dysfunction severity	Diffusion biomarkers	Main results
	Friedli (2017) [53]	27	53 ± 10	Yes	Transplant	Mean GFR = 48 ± 23; CKD G1-4, A1-3	ADC, D, D*, F	Difference between cortex and medulla ADC values (ΔADC) correlated with fibrosis in kidney allograft recipients
	Lanzman (2013) [37]	40	50 ± 15	No	Transplant	Mean eGFR = 49 ± 18 (CKD G1-3, *n* = 23); 17 ± 6 (CKD G4-5, *n* = 17); CKD G1-5, AX	ADC, FA	Medullary FA correlated with eGFR in transplant patients
	Ozcelik (2017) [54]	70	42 ± 12	No	Transplant	Mean eGFR = 74 ± 24; CKD G1-3, AX	ADC	ADC strongly correlated with creatinine and eGFR in transplant patients
	Palmucci (2012) [55]	22	58 (20–79)	No	Transplant	CrCl ≥ 60 (*n* = 13) (30–60) (*n* = 10), ≤30 (*n* = 12); CKD G1-5, AX	ADC	ADC correlated with creatinine clearance in transplant patients
	Palmucci (2015) [56]	30	51 (17–78)	No	Transplant	CrCl ≥ 60 (*n* = 13) (30–60) (*n* = 10), ≤30 (*n* = 12); CKD G1-5 AX	ADC, FA	Medullary ADC best parameter for renal function assessment in transplant patients
Kidney allograft: acute dysfunction	Abou-El-Ghar (2012) [57]	21	28 ± 10	Yes	Transplant: acute cellular rejection (*n* = 10), ATN (*n* = 7), immunosuppressive toxicity (*n* = 4)	Mean srCr = 290 ± 88; acute kidney injury	ADC	DWI is a promising tool for the diagnosis of acute renal transplant dysfunction
	Hueper (2016) [23]	64	54 ± 15	Yes	Transplant: initial graft dysfunction (*n* = 33), delayed graft dysfunction (*n* = 31)	Mean eGFR (at Day 7) = 23 ± 15; delayed graft function	ADC, D, D*, F, FA	Combined DTI and DWI detected allograft dysfunction early after kidney transplantation and correlated with allograft fibrosis
	Park (2014) [25]	24	46 ± 13	Yes	Transplant	Mean srCr = 184 ± 123; acute kidney injury	ADC, (BOLD)	DWI (in combination with BOLD MRI) may demonstrate early functional state of renal allografts, but may be limited in characterizing a cause of early renal allograft dysfunction
	Steiger (2017) [32]	40	59 ± 13	Yes	Transplant	Mean srCr = 258 [85–832]; acute kidney injury	ADC, F, D, D*	Combined qualitative and quantitative DWI might allow to determine the severity of histopathologic findings in biopsies of kidney transplant patients

Fan (2016) [35]	30	40 ± 13	No	Transplant	eGFR = [5–99]; eGFR = (30–60) (n = 19), <30 (n = 11); post allograft	ADC, FA	DTI produces reliable results to assess renal allograft function early after transplantation
Hueper (2011) [33]	15	51 (9–75)	No	Transplant	srCr = (50–563); acute kidney injury	ADC, FA	Changes in allograft function and microstructure can be detected and quantified using DTI
Ren (2016) [58]	62	36 ± 11	No	Transplant	eGFR = 93 ± 15 (eGFR ≥ 60, n = 37), 33 ± 18 (eGFR < 60, n = 25); 2–4 weeks post-allograft	D, D*, F (ASL)	DWI combined with ASL has better diagnostic efficacy in defining renal allograft function

Age is expressed as mean ± SD or mean (range). eGFR and GFR values are in mL/min/1.73 m^2. srCr values are in µmol/L. CKD stage is expressed as KDIGO stage GXAX. IgA, immunoglobulin A; BOLD, blood oxygenation level dependent; ASL, arterial spin labelling; D, diffusion coefficient; D*, pseudodiffusion coefficient; F, flowing fraction; GFR, glomerular filtration rate; CrCl, creatinine clearance; srCr, serum creatinine; sRI, severe renal injury. Only studies performed on at least 15 patients with CKD or kidney allograft dysfunction were included in the table.

and cystic index. A second pilot study using DTI reported higher ADC and lower FA in polycystic kidneys compared with controls but no separation of cystic and non-cystic components was done, precluding the significance of the results [64].

Besides already validated morphological biomarkers of severity of the disease (total cystic and total kidney volumes), new functional biomarkers of NCRP involvement could provide additional insights into kidney characterization and disease progression in patients with polycystic disease.

Obstruction

There are only few publications dealing with DWI in patients with various degrees of ureteral obstruction, with conflicting, but still promising results. In a prospective study including 21 patients with acute unilateral ureteral obstruction, DWI was unable to detect any significant difference in ADC between obstructed and unobstructed kidney [18]. However, the flowing fraction F of the cortex but not the medulla was significantly lower in the obstructed than in the contralateral unobstructed kidney. Contradictory findings were observed in another prospective study performed in a similar setting including 24 patients with a ureteral calculus and a significant reduction in ADC (b-values of 0 and 1000 s/mm^2) could be observed in the obstructed compared with the obstructed kidney [65]. As the non-invasive diagnosis of obstruction is an important clinical challenge, e.g. in pregnant woman, children uteropelvic junction obstruction and transplanted kidneys, further research applying IVIM in these patient groups should be performed in large-scale multicentre trials. Furthermore, non-invasive diagnosis and quantification of obstruction would help in defining the time point of intervention or whether watchful waiting is still possible.

High blood pressure and renal artery stenosis

Non-invasive assessment of the degree of renal artery stenosis with its potential effect on the renal parenchyma might be helpful in decision-making concerning treatment options. There are only a few older studies applying DWI in this context, showing that the ADC mainly in the cortex was significantly lower in kidneys with renal artery stenosis compared with the contralateral kidney or those of healthy volunteers [66, 67]. Applying IVIM, focusing mainly on the flowing fraction F or applying only low b-values might be helpful in improving DWI in this context and prospective studies might be relatively easy to design and perform.

Diabetes

Diabetic kidney disease (DKD) is a common complication of diabetes, the most common form of CKD and the leading cause of end-stage renal disease. Several studies showed lower cortical and medullary ADC values in DKD than in volunteers [15, 51, 52]. Significant correlations were found between mean renal ADC values and clinical stages of DKD [50], and between mean renal ADC values and urinary albumin excretion [50], urinary N-acetyl-beta-D-glucosaminidase, urinary transforming growth factor-beta1 and serum creatinine [52]. In a cohort of early stages of type 2 DKD with or without microalbuminuria,

ADC values were significantly lower in DKD than in controls and medullary FA was significantly higher when macroalbuminuria was present [51]. Increased cortical FA was also reported in two large studies [51, 52], helping in prediction of the presence of macroalbuminuria [52] and being more sensitive than urine albumin excretion rate in reflecting early-stage kidney injury [51].

However, validation of new biomarkers of disease progression and treatment responses is still required. A large cohort of patients with type 2 DKD will be included in a multicentre prospective European protocol of quantitative MRI, including DWI and DTI, to validate new imaging biomarkers allowing to separate slow and fast progressing patients (iBEAT-DKD, IMI call).

CKD

CKD is defined as an alteration of function and/or structure lasting for more than 3 months. The hallmark of structural alteration in CKD is the presence of cortical interstitial fibrosis. Evaluation of kidney cortical interstitial fibrosis is crucial for renal prognosis, early diagnosis and treatment adaptation in CKD since elevation of creatinine is a late phenomenon. DWI currently emerges as one of the most promising tools for kidney fibrosis evaluation in CKD. Although there is debate about the exact modifications observed by DWI, either structural or functional such as related to perfusion modifications [29], DWI can differentiate between a sick and a healthy kidney in experimental but more importantly in human CKD [15, 37, 38, 40, 49, 50, 67, 68, 69]. ADC also correlates with renal function, usually estimated by creatinine values [44, 45, 49, 54, 70, 71]. In the few human studies where histology was available, cortical ADC displayed a good correlation with cortical fibrosis and chronic lesions [28, 38, 39, 53] (Table 3). It remains unclear whether the observed decrease of ADC values is reflecting the decrease of renal function only or the degree of tissue fibrotic changes, or both. Despite these encouraging observations, limitations to the clinical use of DWI in CKD still remain in terms of image resolution, protocol variability and inter-individual variability. In consequence, no clear cut-off of ADC values can be chosen to differentiate CKD versus healthy kidney. Improvement in image resolution providing a better delineation between cortex and medulla should help [53, 72], as well as measuring the difference between cortical and medullary ADC, the so-called delta-ADC, which was shown to decrease inter-individual variability and to be better correlated with fibrosis in CKD [53, 72].

Using DTI, FA was significantly lower in patients with CKD than in healthy controls, regardless of whether estimated glomerular filtration rate (eGFR) was reduced, probably due to changes in the microarchitecture: negative correlations were found between FA and both glomerular lesions and tubulointerstitial injury score [40].

Altogether, DWI could be the imaging technique of choice in all types of CKD, even before renal function declines, to evaluate the degree of tissue fibrosis, to predict renal function evolution and to follow microstructure changes occurring under treatment. This could reduce the number of renal biopsies for diagnosis and follow-up. To become an accepted clinical tool, improvement in DWI reliability and homogenization of acquisition techniques in multicentre studies are crucial.

CONCLUSIONS

DWI is recognized by the scientific community as a powerful imaging biomarker of the renal microstructure with a number of available clinical studies. DWI shows good correlation with renal function decline and with cortical fibrosis in CKD, with a promising monitoring potential. In diffuse renal diseases, DWI could support the decisions to perform renal biopsy and avoid unnecessary interventions. To improve its specificity, DWI is likely to benefit from being combined with other promising MRI modalities (multiparametric MRI) for renal tissue characterization and follow-up, therefore enabling a complete morphological and functional assessment of the normal and diseased kidney [73]. Additional biological validation is needed, as multiple parameters can affect the interpretation of DWI. Furthermore, as current methodological differences across studies hinder a reliable comparison of the results, standardization of acquisition and processing protocols are definitely required, as well as large multicentre studies. The COST action PARENCHIMA, working on standardization of renal MRI techniques, may answer this need.

SUPPLEMENTARY DATA

Supplementary data are available at ndt online.

ACKNOWLEDGEMENTS

This article is based upon work from COST Action Magnetic Resonance Imaging Biomarkers for Chronic Kidney Disease (PARENCHIMA), funded by COST (European Cooperation in Science and Technology). www.cost.eu. For additional information please visit PARENCHIMA project website: www.renalmri.org

FUNDING

J.-P.V., H.C.T. and S.D.S. were partially supported by the Swiss National Foundation (J.-P.V. grant no. 320038_159714, J.-P.V. and H.C.T. grant no. IZCOZ0_177140/1 and S.D.S. grant no. PP00P3_127454). P.B. is supported by the Deutsche Forschungsgemeinschaft (DFG; BO 3755/6-1, SFB/TRR57, SFB/TRR219) and by the German Ministry of Education and Research (BMBF Consortium STOP-FSGS number 01GM1518A).

AUTHORS' CONTRIBUTIONS

A.C. and J.-P.V. contributed to the conception, design, analysis and interpretation of the data, article drafting and revision. M.S. was responsible for data analysis and interpretation, article drafting and revision. I.F. was responsible for data analysis, article revision and figure creation. A.L., L.G. and I.K. were responsible for data analysis and article revision. S.D.S., M.N., H.C.T. and N.G. helped in interpretation of the data,

article drafting and revision. P.B., I.A.M. and N.M.S. helped in interpretation of the data and article revision. All authors provided intellectual content of critical importance and finally approved the version to be published.

CONFLICT OF INTEREST STATEMENT

None declared.

REFERENCES

1. Le Bihan D, Iima M. Diffusion magnetic resonance imaging: what water tells us about biological tissues. *PLoS Biol* 2015; 13: e1002203
2. Stehling MK, Turner R, Mansfield P. Echo-planar imaging: magnetic resonance imaging in a fraction of a second. *Science* 1991; 254: 43–50
3. Damasio MB, Tagliafico A, Capaccio E *et al.* Diffusion-weighted MRI sequences (DW-MRI) of the kidney: normal findings, influence of hydration state and repeatability of results. *Radiol Med* 2008; 113: 214–224
4. Wang WJ, Pui MH, Guo Y *et al.* MR diffusion tensor imaging of normal kidneys. *J Magn Reson Imaging* 2014; 40: 1099–1102
5. Sigmund EE, Vivier PH, Sui D *et al.* Intravoxel incoherent motion and diffusion-tensor imaging in renal tissue under hydration and furosemide flow challenges. *Radiology* 2012; 263: 758–769
6. Yoshikawa T, Ohno Y, Kawamitsu H *et al.* Abdominal apparent diffusion coefficient measurements: effect of diffusion-weighted image quality and usefulness of anisotropic images. *Magn Reson Imaging* 2008; 26: 1415–1420
7. Le Bihan D, Breton E, Lallemand D *et al.* MR imaging of intravoxel incoherent motions: application to diffusion and perfusion in neurologic disorders. *Radiology* 1986; 161: 401–407
8. Wittsack HJ, Lanzman RS, Mathys C *et al.* Statistical evaluation of diffusion-weighted imaging of the human kidney. *Magn Reson Med* 2010; 64: 616–622
9. Zhang JL, Sigmund EE, Chandarana H *et al.* Variability of renal apparent diffusion coefficients: limitations of the monoexponential model for diffusion quantification. *Radiology* 2010; 254: 783–792
10. Ljimani A, Lanzman RS, Muller-Lutz A *et al.* Non-gaussian diffusion evaluation of the human kidney by Pade exponent model. *J Magn Reson Imaging* 2018; 47: 160–167
11. Basser PJ. Inferring microstructural features and the physiological state of tissues from diffusion-weighted images. *NMR Biomed* 1995; 8: 333–344
12. Blondin D, Lanzman RS, Klasen J *et al.* Diffusion-attenuated MRI signal of renal allografts: comparison of two different statistical models. *Am J Roentgenol* 2011; 196: W701–W705
13. Blondin D, Lanzman RS, Mathys C *et al.* [Functional MRI of transplanted kidneys using diffusion-weighted imaging]. *Rofo* 2009; 181: 1162–1167
14. Kataoka M, Kido A, Yamamoto A *et al.* Diffusion tensor imaging of kidneys with respiratory triggering: optimization of parameters to demonstrate anisotropic structures on fraction anisotropy maps. *J Magn Reson Imaging* 2009; 29: 736–744
15. Lu L, Sedor JR, Gulani V *et al.* Use of diffusion tensor MRI to identify early changes in diabetic nephropathy. *Am J Nephrol* 2011; 34: 476–482
16. Notohamiprodjo M, Glaser C, Herrmann KA *et al.* Diffusion tensor imaging of the kidney with parallel imaging: initial clinical experience. *Investig Radiol* 2008; 43: 677–685
17. Ries M, Jones RA, Basseau F *et al.* Diffusion tensor MRI of the human kidney. *J Magn Reson Imaging* 2001; 14: 42–49
18. Thoeny HC, Binser T, Roth B *et al.* Noninvasive assessment of acute ureteral obstruction with diffusion-weighted MR imaging: a prospective study. *Radiology* 2009; 252: 721–728
19. Zhang JL, Sigmund EE, Rusinek H *et al.* Optimization of b-value sampling for diffusion-weighted imaging of the kidney. *Magn Reson Med* 2012; 67: 89–97
20. Gaudiano C, Clementi V, Busato F *et al.* Renal diffusion tensor imaging: is it possible to define the tubular pathway? A case report. *Magn Reson Imaging* 2011; 29: 1030–1033
21. Cheung JS, Fan SJ, Chow AM *et al.* Diffusion tensor imaging of renal ischemia reperfusion injury in an experimental model. *NMR Biomed* 2010; 23: 496–502
22. Wittsack HJ, Lanzman RS, Quentin M *et al.* Temporally resolved electrocardiogram-triggered diffusion-weighted imaging of the human kidney: correlation between intravoxel incoherent motion parameters and renal blood flow at different time points of the cardiac cycle. *Invest Radiol* 2012; 47: 226–230
23. Hueper K, Khalifa AA, Brasen JH *et al.* Diffusion-weighted imaging and diffusion tensor imaging detect delayed graft function and correlate with allograft fibrosis in patients early after kidney transplantation. *J Magn Reson Imaging* 2016; 44: 112–121
24. Friedli I, Crowe LA, Berchtold L *et al.* New magnetic resonance imaging index for renal fibrosis assessment: a comparison between diffusion-weighted imaging and T1 mapping with histological validation. *Sci Rep* 2016; 6: 30088
25. Park SY, Kim CK, Park BK *et al.* Assessment of early renal allograft dysfunction with blood oxygenation level-dependent MRI and diffusion-weighted imaging. *Eur J Radiol* 2014; 83: 2114–2121
26. Derlin T, Gueler F, Brasen JH *et al.* Integrating MRI and chemokine receptor CXCR4-targeted PET for detection of leukocyte infiltration in complicated urinary tract infections after kidney transplantation. *J Nucl Med* 2017; 58: 1831–1837
27. Tourell MC, Powell SK, Momot KI. Diffusion tensor of water in partially aligned fibre networks. *J Phys D Appl Phys* 2013; 46: 455401
28. Zhao J, Wang ZJ, Liu M *et al.* Assessment of renal fibrosis in chronic kidney disease using diffusion-weighted MRI. *Clin Radiol* 2014; 69: 1117–1122
29. Boor P, Perkuhn M, Weibrecht M *et al.* Diffusion-weighted MRI does not reflect kidney fibrosis in a rat model of fibrosis. *J Magn Reson Imaging* 2015; 42: 990–998
30. Donati OF, Chong D, Nanz D *et al.* Diffusion-weighted MR imaging of upper abdominal organs: field strength and intervendor variability of apparent diffusion coefficients. *Radiology* 2014; 270: 454–463
31. Poynton CB, Lee MM, Li Y *et al.* Intravoxel incoherent motion analysis of renal allograft diffusion with clinical and histopathological correlation in pediatric kidney transplant patients: a preliminary cross-sectional observational study. *Pediatr Transplant* 2017; 21: e12996
32. Steiger P, Barbieri S, Kruse A *et al.* Selection for biopsy of kidney transplant patients by diffusion-weighted MRI. *Eur Radiol* 2017; 27: 4336–4344
33. Hueper K, Gutberlet M, Rodt T *et al.* Diffusion tensor imaging and tractography for assessment of renal allograft dysfunction-initial results. *Eur Radiol* 2011; 21: 2427–2433
34. Eisenberger U, Thoeny HC, Binser T *et al.* Evaluation of renal allograft function early after transplantation with diffusion-weighted MR imaging. *Eur Radiol* 2010; 20: 1374–1383
35. Fan WJ, Ren T, Li Q *et al.* Assessment of renal allograft function early after transplantation with isotropic resolution diffusion tensor imaging. *Eur Radiol* 2016; 26: 567–575
36. Li Y, Lee MM, Worters PW *et al.* Pilot study of renal diffusion tensor imaging as a correlate to histopathology in pediatric renal allografts. *AJR Am J Roentgenol* 2017; 208: 1358–1364
37. Lanzman RS, Ljimani A, Pentang G *et al.* Kidney transplant: functional assessment with diffusion-tensor MR imaging at 3T. *Radiology* 2013; 266: 218–225
38. Inoue T, Kozawa E, Okada H *et al.* Noninvasive evaluation of kidney hypoxia and fibrosis using magnetic resonance imaging. *J Am Soc Nephrol* 2011; 22: 1429–1434
39. Li Q, Li J, Zhang L *et al.* Diffusion-weighted imaging in assessing renal pathology of chronic kidney disease: a preliminary clinical study. *Eur J Radiol* 2014; 83: 756–762
40. Liu Z, Xu Y, Zhang J *et al.* Chronic kidney disease: pathological and functional assessment with diffusion tensor imaging at 3T MR. *Eur Radiol* 2015; 25: 652–660
41. Rona G, Pasaoglu L, Ozkayar N *et al.* Functional evaluation of secondary renal amyloidosis with diffusion-weighted MR imaging. *Ren Fail* 2016; 38: 249–255
42. Wang WJ, Pui MH, Guo Y *et al.* 3T magnetic resonance diffusion tensor imaging in chronic kidney disease. *Abdom Imaging* 2014; 39: 770–775
43. Ding J, Chen J, Jiang Z *et al.* Is low b-factors-based apparent diffusion coefficient helpful in assessing renal dysfunction? *Radiol Med* 2016; 121: 6–11
44. Ding J, Chen J, Jiang Z *et al.* Assessment of renal dysfunction with diffusion-weighted imaging: comparing intra-voxel incoherent motion (IVIM) with a mono-exponential model. *Acta Radiol* 2016; 57: 507–512

45. Emre T, Kilickesmez O, Buker A *et al*. Renal function and diffusion-weighted imaging: a new method to diagnose kidney failure before losing half function. *Radiol Med* 2016; 121: 163–172
46. Ichikawa S, Motosugi U, Ichikawa T *et al*. Intravoxel incoherent motion imaging of the kidney: alterations in diffusion and perfusion in patients with renal dysfunction. *Magn Reson Imaging* 2013; 31: 414–417
47. Li Q, Wu X, Qiu L *et al*. Diffusion-weighted MRI in the assessment of split renal function: comparison of navigator-triggered prospective acquisition correction and breath-hold acquisition. *AJR Am J Roentgenol* 2013; 200: 113–119
48. Prasad PV, Thacker J, Li LP *et al*. Multi-parametric evaluation of chronic kidney disease by MRI: a preliminary cross-sectional study. *PLoS One* 2015; 10: e0139661
49. Xu X, Fang W, Ling H *et al*. Diffusion-weighted MR imaging of kidneys in patients with chronic kidney disease: initial study. *Eur Radiol* 2010; 20: 978–983
50. Cakmak P, Yağcı AB, Dursun B *et al*. Renal diffusion-weighted imaging in diabetic nephropathy: correlation with clinical stages of disease. *Diagn Interv Radiol* 2014; 20: 374–378
51. Chen X, Xiao W, Li X *et al*. *In vivo* evaluation of renal function using diffusion weighted imaging and diffusion tensor imaging in type 2 diabetics with normoalbuminuria versus microalbuminuria. *Front Med* 2014; 8: 471–476
52. Razek A, Al-Adlany M, Alhadidy AM *et al*. Diffusion tensor imaging of the renal cortex in diabetic patients: correlation with urinary and serum biomarkers. *Abdom Radiol* 2017; 42: 1493–1500
53. Friedli I, Crowe LA, de Perrot T *et al*. Comparison of readout-segmented and conventional single-shot for echo-planar diffusion-weighted imaging in the assessment of kidney interstitial fibrosis. *J Magn Reson Imaging* 2017; 46: 1631–1640
54. Ozcelik U, Cevik H, Bircan HY *et al*. Evaluation of transplanted kidneys and comparison with healthy volunteers and kidney donors with diffusion-weighted magnetic resonance imaging: initial experience. *Exp Clin Transplant* 2017 [Epub ahead of print]
55. Palmucci S, Mauro LA, Failla G *et al*. Magnetic resonance with diffusion-weighted imaging in the evaluation of transplanted kidneys: updating results in 35 patients. *Transplant Proc* 2012; 44: 1884–1888
56. Palmucci S, Cappello G, Attina G *et al*. Diffusion weighted imaging and diffusion tensor imaging in the evaluation of transplanted kidneys. *Eur J Radiol Open* 2015; 2: 71–80
57. Abou-El-Ghar ME, El-Diasty TA, El-Assmy AM *et al*. Role of diffusion-weighted MRI in diagnosis of acute renal allograft dysfunction: a prospective preliminary study. *Br J Radiol* 2012; 85: e206–e211
58. Ren T, Wen CL, Chen LH *et al*. Evaluation of renal allografts function early after transplantation using intravoxel incoherent motion and arterial spin labeling MRI. *Magn Reson Imaging* 2016; 34: 908–914
59. Vivier PH, Sallem A, Beurdeley M *et al*. MRI and suspected acute pyelonephritis in children: comparison of diffusion-weighted imaging with gadolinium-enhanced T1-weighted imaging. *Eur Radiol* 2014; 24: 19–25
60. Thoeny HC, De Keyzer F. Diffusion-weighted MR imaging of native and transplanted kidneys. *Radiology* 2011; 259: 25–38
61. Faletti R, Cassinis MC, Fonio P *et al*. Diffusion-weighted imaging and apparent diffusion coefficient values versus contrast-enhanced MR imaging in the identification and characterisation of acute pyelonephritis. *Eur Radiol* 2013; 23: 3501–3508
62. Suwabe T, Ubara Y, Ueno T *et al*. Intracystic magnetic resonance imaging in patients with autosomal dominant polycystic kidney disease: features of severe cyst infection in a case-control study. *BMC Nephrol* 2016; 17: 170
63. Kline TL, Edwards ME, Garg I *et al*. Quantitative MRI of kidneys in renal disease. *Abdom Radiol (NY)* 2018; 43: 629–638
64. Lupica R, Mormina E, Lacquaniti A *et al*. 3 Tesla-diffusion tensor imaging in autosomal dominant polycystic kidney disease: the nephrologist's point of view. *Nephron* 2016; 134: 73–80
65. Duzenli K, Ozturk M, Yildirim IO *et al*. The utility of diffusion-weighted imaging to assess acute renal parenchymal changes due to unilateral ureteral stone obstruction. *Urolithiasis* 2017; 45: 401–405
66. Yildirim E, Kirbas I, Teksam M *et al*. Diffusion-weighted MR imaging of kidneys in renal artery stenosis. *Eur J Radiol* 2008; 65: 148–153
67. Namimoto T, Yamashita Y, Mitsuzaki K *et al*. Measurement of the apparent diffusion coefficient in diffuse renal disease by diffusion-weighted echo-planar MR imaging. *J Magn Reson Imaging* 1999; 9: 832–837
68. Thoeny HC, De Keyzer F, Oyen RH *et al*. Diffusion-weighted MR imaging of kidneys in healthy volunteers and patients with parenchymal diseases: initial experience. *Radiology* 2005; 235: 911–917
69. Goyal A, Sharma R, Bhalla AS *et al*. Diffusion-weighted MRI in assessment of renal dysfunction. *Indian J Radiol Imaging* 2012; 22: 155–159
70. Carbone SF, Gaggioli E, Ricci V *et al*. Diffusion-weighted magnetic resonance imaging in the evaluation of renal function: a preliminary study. *Radiol Med* 2007; 112: 1201–1210
71. Yalçin-Şafak K, Ayyildiz M, Ünel SY *et al*. The relationship of ADC values of renal parenchyma with CKD stage and serum creatinine levels. *Eur J Radiol Open* 2016; 3: 8–11
72. Friedli I, Crowe LA, Viallon M *et al*. Improvement of renal diffusion-weighted magnetic resonance imaging with readout-segmented echo-planar imaging at 3T. *Magn Reson Imaging* 2015; 33: 701–708
73. Cox EF, Buchanan CE, Bradley CR *et al*. Multiparametric renal magnetic resonance imaging: validation, interventions, and alterations in chronic kidney disease. *Front Physiol* 2017; 8: 696

Received: 30.4.2018; Editorial decision: 2.5.2018